



Comparative study of alkali roasting and leaching of chromite ores and titaniferous minerals



Stephen Parirenyatwa ^{*}, Lidia Escudero-Castejon ^{*}, Sergio Sanchez-Segado, Yotamu Hara, Animesh Jha

Institute of Materials Research, Houldsworth Building, University of Leeds, Leeds LS2 9JT, UK

ARTICLE INFO

Article history:

Received 15 June 2015

Received in revised form 30 July 2015

Accepted 9 August 2015

Available online 13 August 2015

Keywords:

Alkali roasting

Titanium

Chromium

Ilmenite

Chromite

Organic acid leaching

ABSTRACT

Extraction of titanium and chromium oxides may be achieved via roasting the respective minerals with alkali at high temperatures, followed by water and organic acid leaching. In this study, sodium and potassium hydroxides are used as alkali for roasting of chromite ores and ilmenite mineral concentrates. The thermodynamic analysis of the roasting process is discussed in terms of designing the process. Samples of chromite and titaniferous minerals were roasted with NaOH and KOH in a temperature range of 400 °C–1000 °C in an oxidising atmosphere. The roasted chromite and ilmenite samples were further processed in order to extract water-soluble Na₂CrO₄ from the reacted chromite and purify titanium dioxide from titaniferous minerals, respectively. The TiO₂ purity obtained after roasting at 400 °C with NaOH and double leaching was 49.2 wt.%, whereas when using KOH the purity was 54.5 wt.%. The highest TiO₂ purity obtained after roasting at 1000 °C for 2 h and double leaching with water and organic acids was 84 wt.%. At low temperature (400 °C) the recovery of chromium was higher for chromite roasted with KOH than for chromite roasted with NaOH. However, at high temperatures (700 °C and 1000 °C) chromium recoveries were similar when roasting with both hydroxides. Around 95% chromium extraction yield was achieved when chromite was roasted with sodium and potassium hydroxides at 1000 °C for 2 h and water leached.

© 2015 The Authors. Published by Elsevier B.V. This is an open access article under the CC BY license (<http://creativecommons.org/licenses/by/4.0/>).

1. Introduction

For the last 40 years, global economic growth has resulted in a rapid increase in the demand for a range of metals and metal oxides for high technology applications, including titanium dioxide (TiO₂) and chromium oxide (Cr₂O₃) (Brown et al., 2015). This has led to a rise in the consumption of their mineral oxides, TiO₂ and Cr₂O₃, derived from ilmenite and chromite, respectively. As a consequence, the amount of waste generated and the energy required to treat the mineral feedstock has placed an increasing strain on the global environment. The world total production of titaniferous minerals and chromite ores and concentrates for the period 1971–2013, in millions of metric tonnes, is compared in Fig. 1.

Bearing the fact that the environment burden on industry is increasing, research must focus on the development of alternative processing routes, which alleviate the problem of wastes, materials and energy, by reducing the time for processing and reducing the waste volume at the end of the process. One of the reasons why we have undertaken comparative studies of chromite ore and titaniferous minerals is that often small concentrations of chromium oxide (0.1 to 0.5 wt.%) are found in ilmenite, and TiO₂ in chromite deposits, especially from S.

Africa. The presence of Ti metal as an impurity in Cr for steel making is undesirable, and also the strong green colour of Cr³⁺ in TiO₂ is not acceptable. For this reason, in this article a novel approach, based on alkali roasting at moderately high temperatures followed by leaching at low temperatures has been investigated for the treatment of titanium oxide minerals and chromium ores. The present work is focussed on studying the physico-chemical changes that occur during the alkali roasting of ilmenite mineral concentrates and chromite ores, using sodium and potassium hydroxides. The thermodynamics of alkali roasting for both minerals is also analysed by computing Gibbs energies of relevant reactions.

1.1. Production of TiO₂ from ilmenite mineral

Titanium is found in nature in a large variety of minerals of which ilmenite (FeTiO₃), rutile (TiO₂), anatase (TiO₂), brookite (TiO₂), perovskite (CaTiO₃) and leucosene (Fe₂O₃·TiO₂) are the most representative (Habashi, 1997). Even though the demand for titanium metal from the energy and chemical industries is expected to increase during the next 10 years, the largest share (90%) of the titanium product market is still dominated by the paint and pigment industry, which requires white TiO₂ (Kogel, 2006). Ilmenite is the main feedstock for the extraction of TiO₂ pigment via the sulphate process, but increasingly the chloride process, which uses rutile or high-grade titanium slag, is being favoured due to the fact that it appears to be more favourable in terms of cost

^{*} Corresponding author.

E-mail addresses: pm12sp@leeds.ac.uk (S. Parirenyatwa), pmllec@leeds.ac.uk (L. Escudero-Castejon).

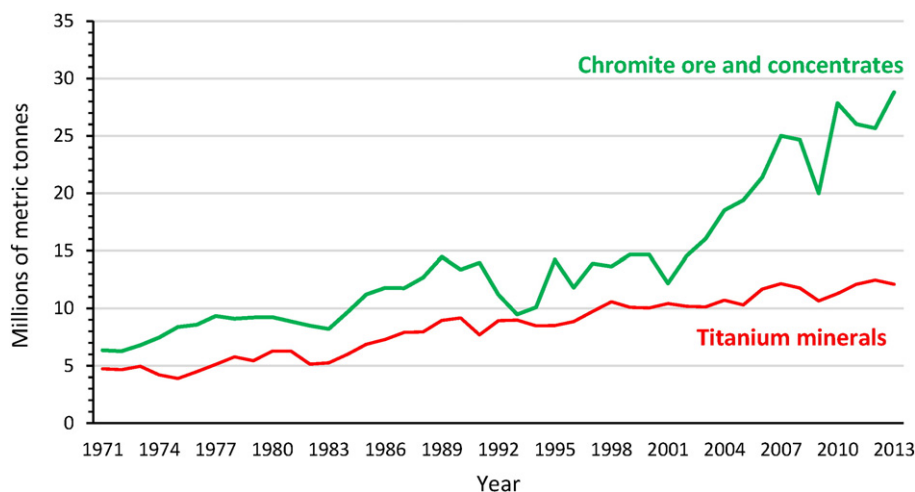


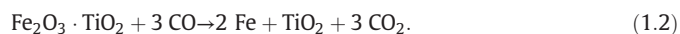
Fig. 1. World total output of titanium oxide based minerals and chromite ores and concentrates from 1971 to 2013. Brown et al. (2015).

and waste management, when compared to the sulphate process (Rosenbaum, 1982). However, due to the limited supply of natural rutile and increasing usage of the chloride process, it has become necessary to produce synthetic rutile by upgrading ilmenite (Mackey, 1994).

Several processes exist for the upgrading of ilmenite, with the Becher process being an example of one employed on a commercial scale (Zhang et al., 2011). In the Becher process, ilmenite is pre-oxidised in air to form pseudobrookite ($\text{Fe}_2\text{O}_3 \cdot \text{TiO}_2$) and TiO_2 , converting the Fe^{2+} ions to Fe^{3+} ions. This follows reaction (1.1):



The pre-oxidised ilmenite is reduced with coal at 1200 °C in a rotary kiln, converting the iron oxide to metallic iron:



The metallic iron is oxidised and precipitated using an aeration process where ammonium chloride is used as a catalyst (Farrow et al., 1987). After the removal of precipitated iron, any remaining iron is removed by leaching with sulphuric acid, leaving behind synthetic rutile with around 93 wt.% TiO_2 (Becher et al., 1965; Filippou and Hudon, 2009):



Indeed the Becher process involves high-temperature oxidation, followed by metallisation and then leaching. The iron derived is not available in a suitable metallic form for iron or steelmaking.

Alkali treatment of ilmenite and titanium bearing ores at high temperatures has been extensively studied. This includes work by Foley and MacKinnon (1970) that involved roasting of ilmenite with potassium and sodium carbonates, at 860 °C, and subsequent leaching of the alkali titanates formed, with hydrochloric acid (HCl). Kinetics and reaction mechanism of soda ash roasting of ilmenite, in the 600 °C–900 °C temperature range, was studied by Lahiri and Jha (2007). Sanchez-Segado et al. (2015a) further studied alkali roasting of Bomar ilmenite with sodium, potassium and lithium carbonates and hydroxides, followed by acid leaching in order to produce synthetic rutile. They were able to achieve 97% pure TiO_2 from a feedstock containing 75% TiO_2 , after leaching for 5 h. Further studies have focussed on direct leaching of ilmenite in aqueous solutions of potassium or sodium hydroxide and followed by acid leaching. Nayl and Aly (2009) decomposed ilmenite in an aqueous solution of KOH and investigated

this route by using a range of acids to produce high-grade TiO_2 . Amer (2002) pressure-leached ilmenite at a high temperature with NaOH before leaching with HCl to produce high-grade TiO_2 . Lahiri and Jha (2009) roasted ilmenite with KOH and were able to selectively separate the rare earths that were present. Manhique et al. (2011) investigated the roasting of ilmenite with NaOH at different temperatures but no comparison was made with other alkali salts.

1.2. Chromium extraction from chromite ore

Chromium is present in many different minerals, nevertheless, just chromite ore, which can be expressed with the general formula $(\text{Fe}_a\text{Mg}_{(1-a)})(\text{Cr}_b\text{Al}_{(1-b)})_2\text{O}_4$, is used for commercial extraction of chromium (Maliotis, 1996). Chromites often have up to 1.5% TiO_2 , with Ti ions occupying octahedral sites in the spinel structure. Chromium compounds are widely used in manufacturing of metals and production of chromium-based chemicals and refractory materials (Ding and Ji, 2003). The estimated world production of chromite ore in 2014 was 29 million metric tonnes (Brown et al., 2015). The global resources of shipping-grade chromite are more than 12 billion tonnes, with about 95% of them located in Southern Africa and Kazakhstan (U.S. Geological Survey, 2015). Chromium is an important alloying element for increasing the oxidation resistance of iron and nickel in high-alloy steels and super alloys. Different chromium chemicals are also used as pigments, in electroplating, as mordant in the leather industry and for manufacturing of refractory materials.

Current technologies for chromite ore processing present serious environmental problems associated with waste disposal. Previous research reported that around 15 wt.% of chromium oxide present in chromite does not react in traditional alkali roasting process, which then generates a chromite ore processing residue (COPR) containing about 0.1 to 0.2 wt.% Cr^{6+} . Landfilling is the traditional method of waste disposal and has become a significant source of hazardous hexavalent chromium (Antony et al., 2001). Various processes such as soda-ash roasting (Antony et al., 2001), acid leaching (Geveci et al., 2002; Zhao et al., 2014), alkali leaching (Xu et al., 2005; Zhang et al., 2010) and alkali fusion (Hundley et al., 1985) have been developed for the processing of chromite ores in order to produce sodium chromate (Na_2CrO_4), which is the primary product used for the manufacturing of different chromium chemicals. Because of economic and technical reasons, just soda-ash roasting has been used worldwide on a commercial scale, either in a rotary kiln or in a rotary hearth furnace. In this process, the extraction of chromium is achieved via roasting the mineral with alkali salts (usually sodium carbonate). Chromite ore and sodium carbonate are roasted at temperatures ranging between 900 °C and

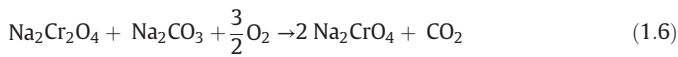
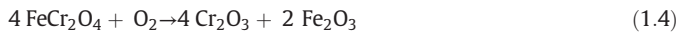
Table 1

Analysis of the as-received mineral concentrates and ores. Chemical composition was analysed by XRF. Both phase analysis and lattice parameter determinations were carried out by X-ray powder diffraction technique, using $\text{CuK}\alpha$ radiation.

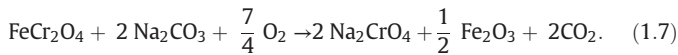
Chemical composition (wt.%)	Chromite ore	Ilmenite concentrate
	wt.%	wt.%
Cr_2O_3	48.80	–
Fe_2O_3	31.30	44.50
MgO	7.03	–
Al_2O_3	7.15	0.91
SiO_2	3.45	0.59
CaO	0.54	–
TiO_2	0.70	51.20
V_2O_5	0.31	0.34
MnO	0.29	1.48
ZrO_2	–	0.29
Lattice parameter (Å)	$a = 8.1983$	$a = 5.088$ $c = 14.076$
Particle size (μm)	106	106
Phases analysis	$(\text{Fe}_{0.52}\text{Mg}_{0.48})(\text{Cr}_{0.76}\text{Al}_{0.24})_2\text{O}_4$ $\text{Ca}_{11.5}\text{Al}_{23}\text{Si}_{25}\text{O}_{96}\text{SiO}_2$	FeTiO_3 , $\text{Fe}_2\text{Ti}_3\text{O}_9$, $\text{Ti}_{0.984}\text{Al}_{0.016}\text{O}_{1.992}$

1200 °C in oxidative atmosphere (Antony et al., 2001). Under these conditions, chromium is oxidised to Cr^{6+} state, which then solubilises in water in the form of alkali chromate (e.g. Na_2CrO_4).

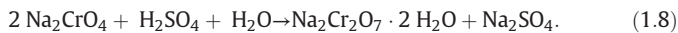
The three main reactions occurring during soda-ash roasting are:



and the overall reaction may be expressed as:



Sodium chromate formed during roasting is selectively leached out with water from the roasted calcine. The residue after water leaching is a Fe and Mg-rich phase which also contains trapped hexavalent chromium. This residue needs to be landfilled which inevitably represents a hazardous source of hexavalent chromium, being considered highly toxic and hazardous for human beings and the environment (Nickens et al., 2010). Sodium dichromate is produced from sodium chromate solutions by acidification with sulphuric acid and further crystallisation (Arslan and Orhan, 1997).



The addition of lime to the soda-ash roasting of chromite solved some technical problems of the traditional roasting process, improving therefore its efficiency. The addition of lime enables the neutralisation of silica by forming silicates, enhancing the oxygen diffusion and reducing the amount of alkali consumed. On the other hand, the formation of highly volatile calcium chromate (CaCrO_4) contributes to air-borne Cr^{+6}

pollution and reduces the process efficiency. These are the main limitation of the lime process (Kowalski and Gollinger-Tarajko, 2003).

Much later the lime-free process was developed, which is able to overcome the environmental problems associated with CaCrO_4 . Nowadays, the lime-free technology has been industrially adopted in most developed countries as an alternative to a dolomite-based process. However, it is limited to ores with silica content lower than 1% (Maliotis, 1996) due to its negative effect on the oxygen transport at the reaction interface.

Much research work has been carried out in an attempt to: optimise the process parameters of alkali roasting of chromite ore and establish the kinetics and the mechanisms of the reaction (Te'pish and Vil'nyanskii, 1969; Tathavadkar et al., 2001, 2003; Antony et al., 2006; Sanchez-Segado and Jha, 2013). Maximising the yield of sodium chromate is therefore the main challenge, for both economic and environmental aspects associated with the manufacturing of chromium compounds from chromite ores. In this paper we aim to maximise the extraction yield of Cr^{6+} from alkali roasted minerals.

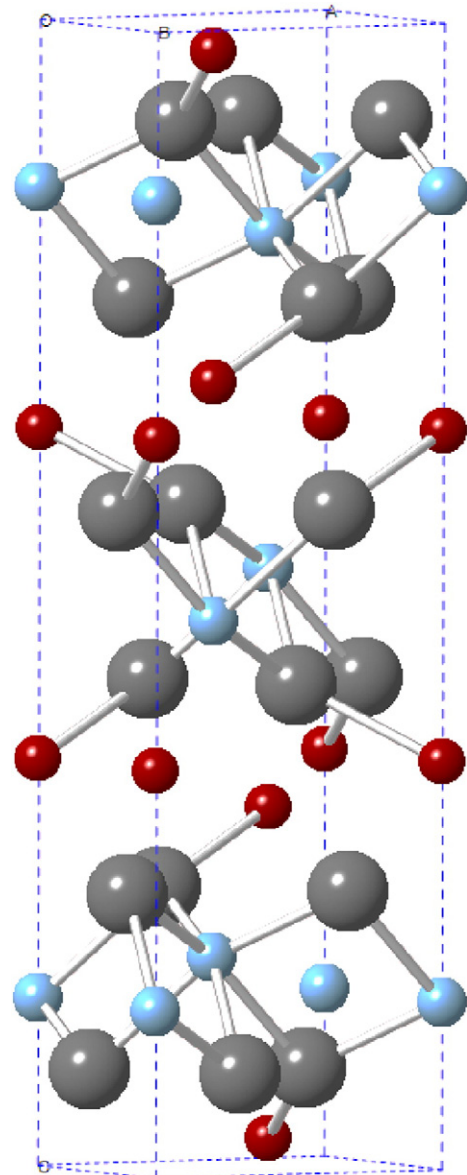


Fig. 2. Crystal structure of ilmenite mineral (O = grey, Ti = blue, Fe = red).

Table 2

Summary of roasting experiments of ilmenite and chromite ores using MOH = NaOH/ KOH as alkali.

Experiment	Molar ratio		Alkali salt	Roasting temperature (°C)
	$\text{Cr}_2\text{O}_3:\text{MOH}$	$\text{TiO}_2:\text{MOH}$		
A	1:7.8	1:3.8	NaOH	400
B	1:7.8	1:3.8	NaOH	700
C	1:7.8	1:3.8	NaOH	1000
D	1:7.8	1:3.8	KOH	400
E	1:7.8	1:3.8	KOH	700
F	1:7.8	1:3.8	KOH	1000

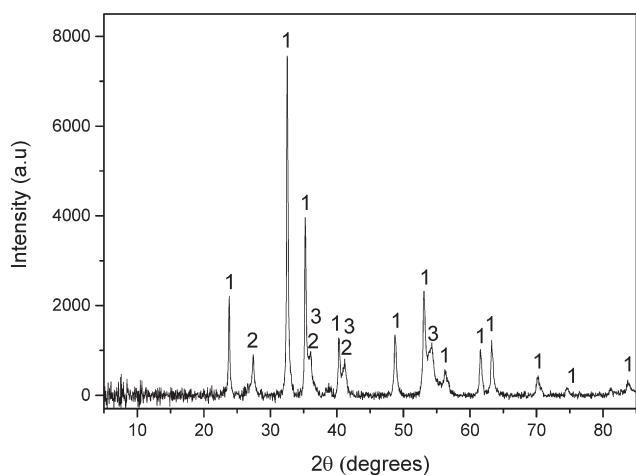


Fig. 3. X-ray diffraction pattern of ilmenite concentrate: 1 = FeTiO_3 (01-075-1209), 2 = $\text{Fe}_2\text{Ti}_3\text{O}_9$ (00-019-0635), 3 = $\text{Ti}_{0.984}\text{Al}_{0.016}\text{O}_{1.992}$ (04-008-2608). The data are compared with the ICDD references in brackets.

2. Experimental

2.1. Ores and reagents

South African chromite and ilmenite ores were used in this study. The X-ray fluorescence (XRF) analysis of the as-received ilmenite and chromite ores are presented in Table 1. Physico-chemical characterisation of the ores is discussed in further detail in the Results and discussion section. Reagent and chemical grades of NaOH, KOH, oxalic acid and ascorbic acid were used in this investigation.

2.2. Experimental setup

All roasting experiments were performed in an electrically heated stainless-steel tube furnace where the temperature was controlled by a programmable temperature-controlling device. For every experiment, known amounts of mineral and alkali salt (NaOH or KOH) were mixed by grinding and placed in a cylindrical alumina crucible. The molar ratios used are shown in Table 2. Samples were isothermally roasted in air atmosphere at a fixed temperature ranging from 400 °C to 1000 °C depending on the experiment.

A first set of alkali roasting experiments was carried out using NaOH and KOH, in which the roasting temperatures 400 °C, 700 °C and 1000 °C were investigated. A summary of these experiments is presented in Table 2.

Table 3
Elemental composition of areas A and B in Fig. 4b analysed by SEM-EDX.

%wt.	Ti	Fe	O	Mn	Al
A	49.5	13.3	35.7	–	1.2
B	33.6	36.8	27.9	1.0	0.7

All chromite roasted samples were leached in water for 2 h at 60 °C with continuous stirring. Roasted ilmenite samples were treated in a two-stage leaching process, where the first step involved water leaching and this was followed by organic acid (mixture of 0.25 M oxalic and 0.01 M ascorbic acid) leaching for 2 h, so as to obtain TiO_2 -rich residue. During the acid leaching, the leachates were sampled at different times for chemical analysis by atomic absorption spectroscopy (AAS).

In a different set of experiments, chromite samples were roasted at different times (15 min–2 h) with excess NaOH and KOH at 1000 °C. These samples were water leached and the remaining residues were analysed.

2.3. Characterisation techniques

After roasting and leaching, the powder samples were analysed using a Philips X'Pert X-ray diffractometer. Samples were analysed over an angle 2θ with a maximum range of 5 to 85°, using $\text{Cu-K}\alpha$ radiation. X'Pert HighScore Plus database software was used for phase-identification of the XRPD patterns obtained. Scanning electron microscopy (SEM) including the use of energy-dispersive X-ray spectrometry (EDX) was used to study the microstructure. X-ray fluorescent diffraction (XRF) was employed for analysing the chemical composition of solid samples. The leachates from acid leaching after roasting ilmenite were analysed by atomic absorption spectroscopy (AAS).

3. Results and discussion

3.1. Ore characterisation

3.1.1. Characterisation of ilmenite ore

Ilmenite has a hexagonal structure containing two cations, titanium and iron, which form alternating bilayers perpendicular to the c axis (Wilson et al., 2005). Fe^{2+} and Ti^{4+} ions are tetrahedrally and octahedrally coordinated, respectively with the O ions. As shown above in Table 1, the ilmenite mineral contains manganese, which generally exists as a substitutional impurity for Fe^{2+} . In the ilmenite lattice both Fe^{2+} and Fe^{3+} can exist, which may be partially or completely substituted by Mn^{2+} and Mn^{3+} , respectively. This is because the size difference between Fe^{2+} (0.92 Å) and Mn^{2+} (0.97 Å) is less than 15%, which means that extensive ionic substitution may be

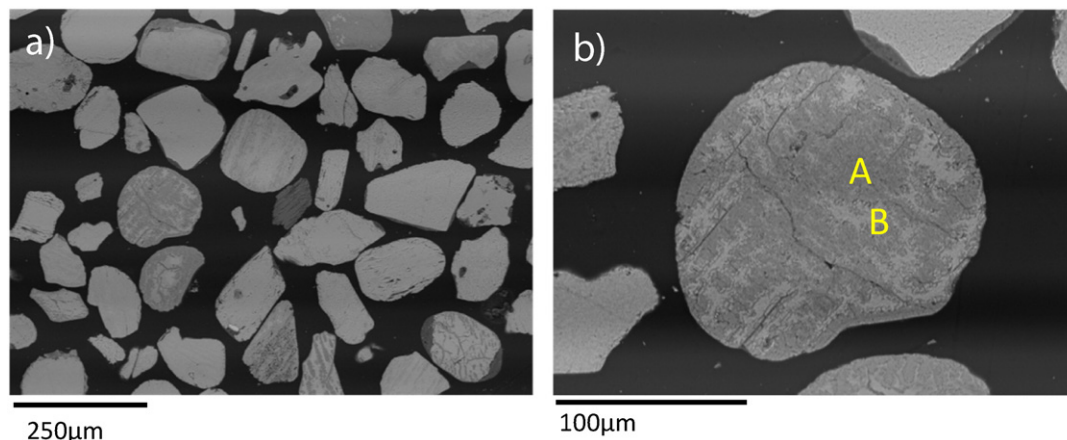


Fig. 4. Backscattered scanning electron microscopy image of ilmenite: a) low-magnification image and b) EDX elemental analysis.

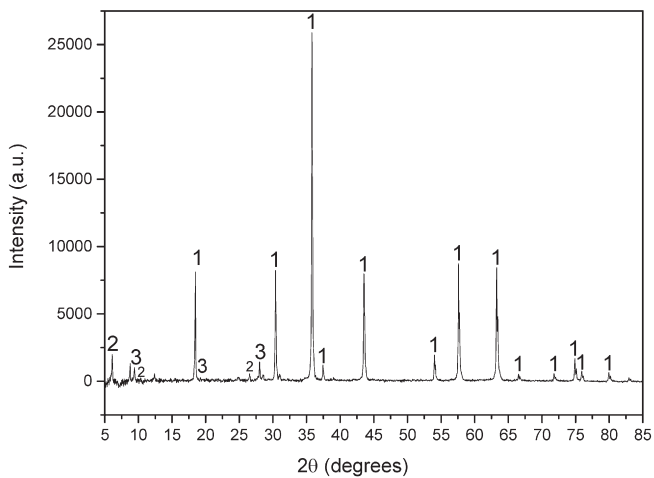


Fig. 5. X-ray powder diffraction pattern of chromite ore. 1 = $(\text{Fe}_{0.52}\text{Mg}_{0.48})(\text{Cr}_{0.76}\text{Al}_{0.24})_2\text{O}_4$ (01-070-6387), 2 = $\text{Ca}_{1.5}\text{Al}_{2.3}\text{Si}_{2.5}\text{O}_{9.6}$ (04-009-9842), 3 = SiO_2 (01-073-3423). The data are compared with the ICDD references in brackets.

possible between these two ions (Klein and Philpotts, 2012). The crystal structure of ilmenite mineral is presented in Fig. 2.

An example of the powder diffraction pattern of ilmenite concentrate is shown in Fig. 3. The main phases identified therein are ilmenite, pseudorutile ($\text{Fe}_2\text{Ti}_3\text{O}_9$) and titanium aluminium oxide, with ilmenite being the dominant phase.

Backscattered scanning electron microscopy (SEM) images of the as-received ilmenite sample are presented in Fig. 4. Analysis of these images shows that the main phase present is FeTiO_3 , which confirms the XRPD data in Fig. 3. The SEM analysis confirms the presence of manganese as a solid solution with the ilmenite phase. Cross-sectional analysis of individual particles, as exemplified in Fig. 4a, shows that there are titanium-rich and iron-rich areas. Dark-grey phase (area A in Table 3) is rich in titanium. This represents the pseudorutile phase which forms during weathering of ilmenite, as identified by Teufer and Temple (1966). The presence of pseudorutile confirms the evidence for weathering of ilmenite, in which the ferrous iron is oxidised to a ferric state. One-third of such iron is leached out, forming the pseudorutile (Grey and Reid, 1975) as shown in Fig. 3. Weathering also leads to the depletion of manganese. Analysis of the light grey phase (area B in Table 3) reveals that the composition of this phase is consistent with that of ilmenite. Fig. 4a is a low magnification image of ilmenite which shows that the predominant phase is ilmenite, with some weathered ilmenite also present.

Table 4
Elemental composition of areas A to D in Fig. 6 analysed by SEM–EDX.

wt.%	Cr	Fe	O	Mg	Al	Si	Ca	Na	Ti
A	36.8	21.8	27.3	5.8	7.9	–	–	–	0.5
B	36.7	22.8	26.6	5.7	7.7	–	–	–	0.5
C	0.6	0.4	41.0	–	18.9	24.3	13.0	1.8	–
D	37.1	22.4	25.8	6.2	8.0	–	–	–	0.4

3.1.2. Characterisation of chromite ore

Chromium is present in complex oxide minerals, occasionally combined with iron oxides and other transition metal oxides such as manganese, titanium, vanadium, niobium and tantalum (Sanchez-Segado et al., 2015b). Chromite ore belongs to the spinel group with the general chemical formula of XY_2O_4 , where X and Y represent divalent and trivalent metal ions, respectively. Chromite has an ideal composition of FeCr_2O_4 , however, the natural mineral is usually represented by the general formula $(\text{Fe}^{2+}, \text{Mg})(\text{Cr}, \text{Al}, \text{Fe}^{3+})_2\text{O}_4$, with sometimes small quantities of Mn, Ti and V included in the crystal structure. The X-ray powder diffraction pattern of the as-received chromite mineral used in the present study can be seen in Fig. 5. The main phase observed is the chromite phase with Fe and Mg as divalent cations and Cr and Al as trivalent cations. Free silica and complex calcium and aluminium silicates are found along with chromite particles as impurities.

According to the rule of parsimony stated by Linus Pauling in 1929 (Pauling, 1929), some mineral structures may need to locate a certain number of ions while they tend to have limited different atomic positions within the crystal lattice. As a consequence, when a mineral has a complex composition with limited structural positions chemical elements substitute for each other in specific atomic sites, giving as a result what is called solid solution (Klein and Philpotts, 2012). This is applicable to chromite minerals, which is a solid solution of four different spinels from a combination of the following potential end members: FeAl_2O_4 , MgAl_2O_4 , FeCr_2O_4 , MgCr_2O_4 , Fe_3O_4 and MgFe_2O_4 . A range of combinations of solid solution therefore emerges, which coexist in a given ore body. From the XRPD pattern in Fig. 5, the chromite ore used in this study may be described by the spinel solid-solution formula $(\text{Fe}_{0.52}\text{Mg}_{0.48})(\text{Cr}_{0.76}\text{Al}_{0.24})_2\text{O}_4$. The composition of the chromite may vary due to replacement of cations with a comparative size, resulting in differing chemical compositions and mineralogical properties based on geographic location (Tathavadkar et al., 2004).

The chemical composition of South African chromite, presented in Table 1, is considered to be of chemical grade, as it has high chromium content (48.8 wt.% Cr_2O_3) and a Cr:Fe weight ratio of 1.52:1 (with 1.5–2:1 being the required ratio). Even though the silica content is not high (3.45 wt.% SiO_2), less than 1% silica content is desirable for chemical

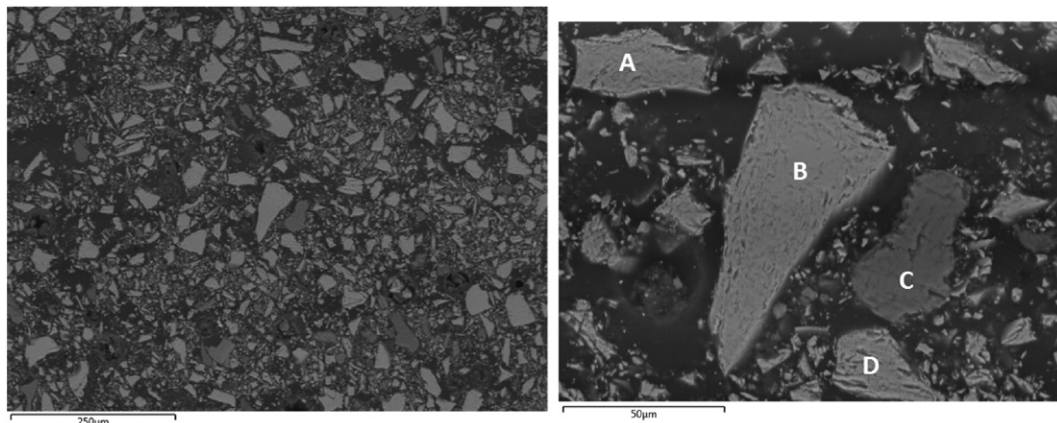


Fig. 6. Backscattered scanning electron microscopy images of the as-received chromite ore: low magnification (left) and high magnification (right).

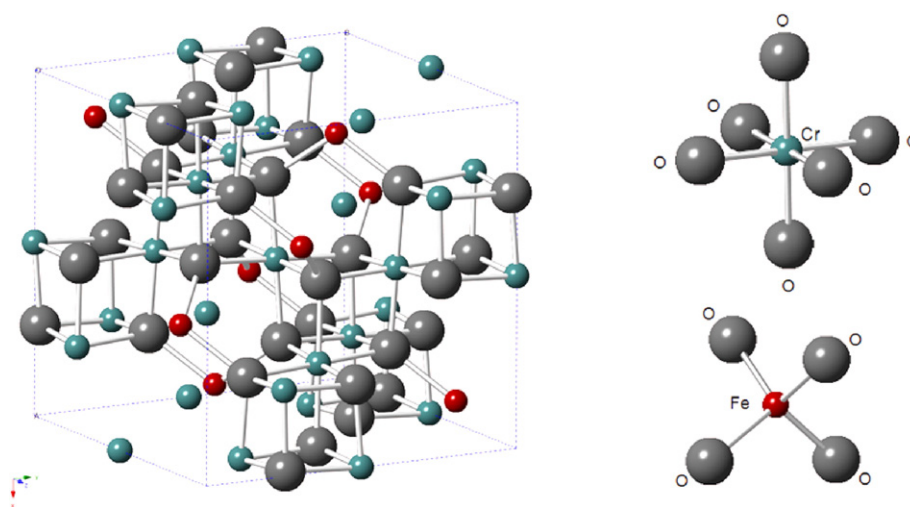


Fig. 7. Crystal structure of chromite ore (O = grey, Fe = red, Cr = green).

grade chromites (Maliotis, 1996) so as to reduce the formation of alkali and alkaline earth silicates.

A backscattered SEM image of the as-received chromite is shown in Fig. 6. Two phases can be clearly differentiated: light grey particles (A, B, D) and slightly darker grey particles (C) corresponding to chromite spinel and siliceous gangue particles, respectively. The EDX-SEM elemental analysis of areas A–D are shown in Table 4, from which it is evident that the composition of chromite ore is fairly uniform on microscopic scale and does not vary significantly from one particle to another. The gangue phase is mainly composed of silica combined with aluminium and calcium, which agrees with XRPD results in Fig. 5.

From a crystal structure view point the chromite spinel is considered a complex mixed-crystal system with oxygen atoms arranged in a face centred cubic close-packed spinel lattice. Within one spinel unit cell, containing eight formula units, there are eight divalent cations ($X^{2+} = \text{Fe}^{2+}, \text{Mg}^{2+}$) occupying tetrahedral positions and 16 trivalent cations ($Y^{3+} = \text{Cr}^{3+}, \text{Al}^{3+}, \text{Fe}^{3+}$) octahedrally coordinated with oxygen (Burns, 1993). The crystal structure of chromite can be seen in Fig. 7.

Treatment of chromite and ilmenite by alkali roasting is highly influenced by the mineralogy and chemical composition of the ore (Tathavadkar et al., 2004), thus the characterisation of the mineral is a critical step. In the majority of chromite ores from South Africa, the ilmenite mineral is present in the solid solution form, which is possible due to the small size differences amongst the participating cations (Tathavadkar et al., 2004). In such complex spinels, the Ti^{4+} ions tend to substitute for the Cr^{3+} or Al^{3+} at octahedral sites, due to the large site preference energy of Ti in (4+) valence state, when compared with Cr^{3+} at the same site.

3.2. Thermodynamics

3.2.1. Thermodynamic study of alkali roasting of ilmenite

Alkali roasting of ilmenite in an oxidising atmosphere results in the conversion of iron from Fe^{2+} to Fe^{3+} . The reactions that may occur during roasting of ilmenite with KOH and NaOH are compared in Eqs. (3.1) and (3.2) and the computed Gibbs energy (ΔG) calculations are plotted against temperature in Fig. 8 (Roine and Outokumpu, 2002). From the Gibbs energy plots (Fig. 8), it is evident that both

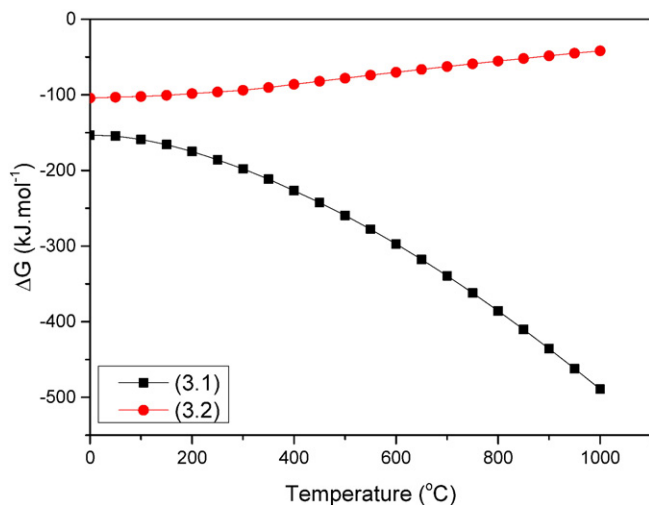


Fig. 8. Comparison of free energy vs temperature curves for reactions (3.1) and (3.2). Values calculated using HSC 5.1 software.

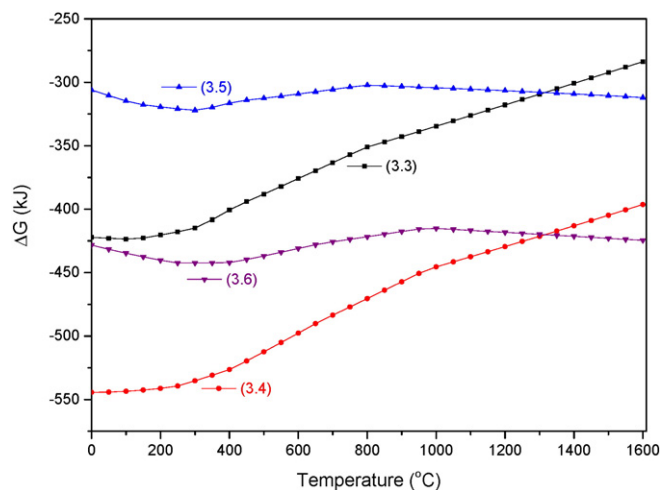


Fig. 9. Comparison of free energy vs temperature curves for reactions (3.3) to (3.6). Values calculated using HSC 5.1 software.

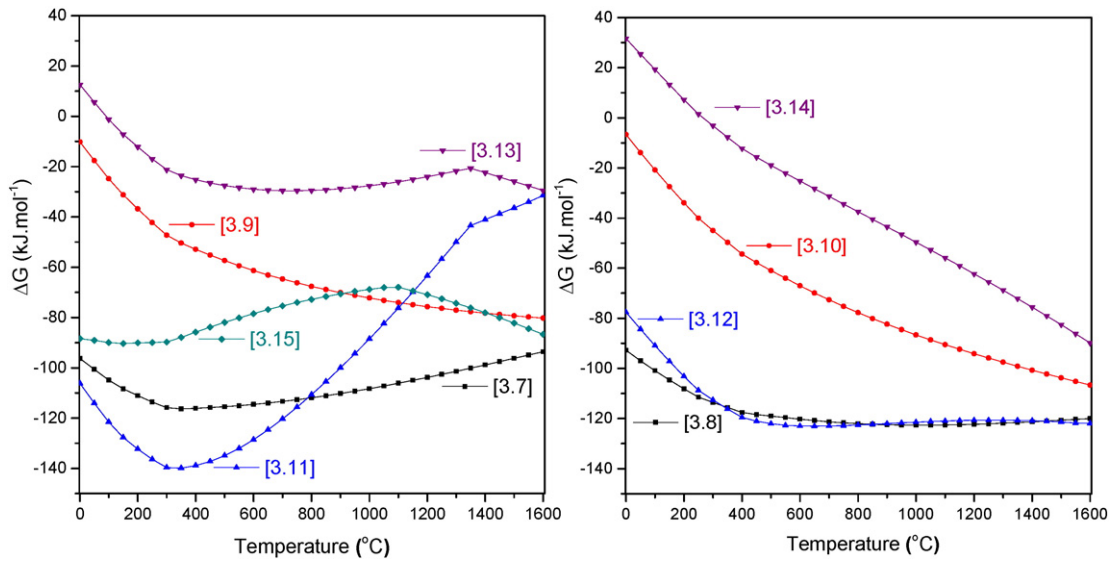
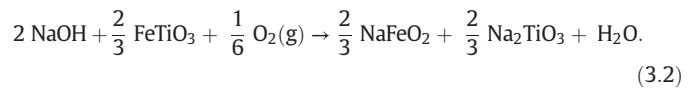
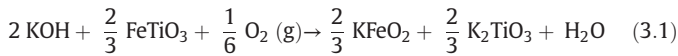


Fig. 10. ΔG versus temperature plots of reactions (3.7)–(3.15). Values calculated using HSC 5.1 software.

reactions are thermodynamically favourable in the experimental operating range (400 °C to 1000 °C). Reaction (3.1) is more favourable than the reaction (3.2). Reaction (3.2) becomes slightly more positive as the temperature increases, whereas reaction (3.1) becomes significantly more negative. This means that from the ΔG calculation it can be concluded that the formation of potassium titanate (K₂TiO₃) is thermodynamically more favourable than the formation of sodium titanate (Na₂TiO₃).



3.2.2. Thermodynamic study of alkali roasting of chromite

During roasting of chromite ore with NaOH/KOH in the presence of oxygen, chromium is oxidised from Cr³⁺ to Cr⁶⁺ and reacts with alkali to form chromate compounds. Both sodium and potassium chromates (Na₂CrO₄, K₂CrO₄) are water-soluble and hence can be extracted from the roasted samples by water leaching. The reaction chemistry of

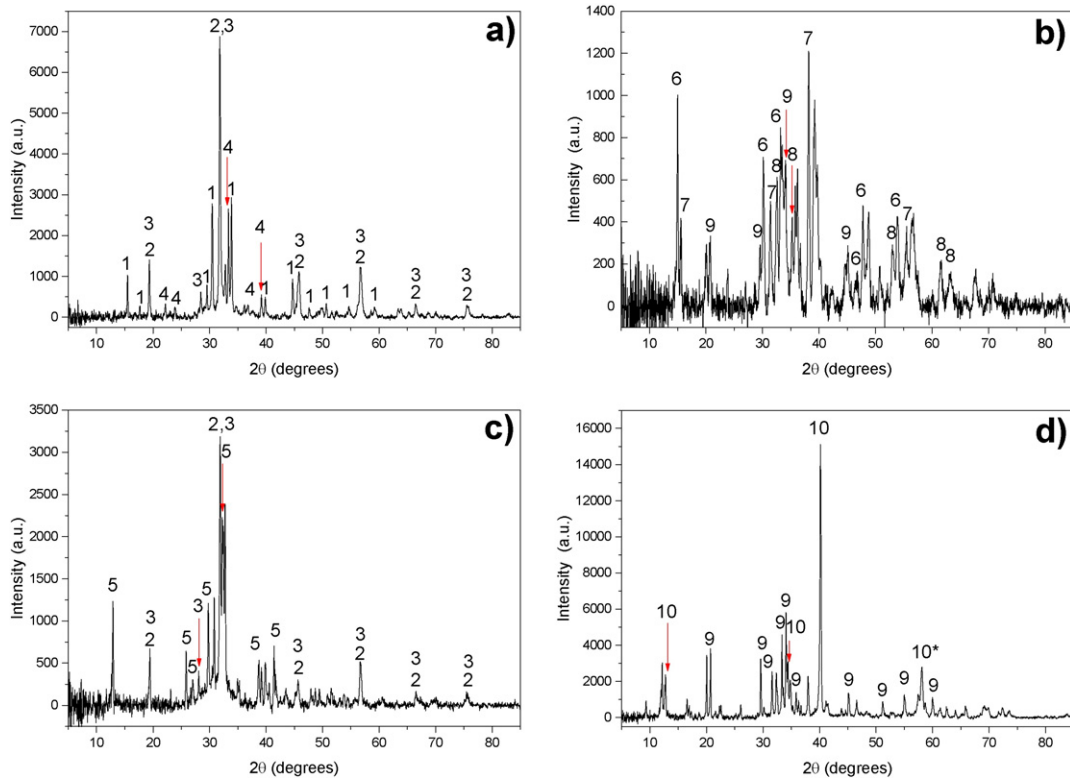


Fig. 11. X-ray powder diffraction pattern of roasted ilmenite with a) KOH at 400 °C, b) NaOH at 400 °C, c) KOH at 700 °C and d) NaOH at 700 °C. 1 = K₂TiO₃ (00-018-1045), 2 = K_{0.85}Fe_{0.85}Ti_{0.15}O₂ (00-062-0213), 3 = KFeO₂ (00-026-1319), 4 = KOH (00-001-1054), 5 = K₂TiO₃ (00-001-1016), 6 = NaOH.H₂O (00-003-0089), 7 = NaOH (01-078-0188), 8 = FeTiO₃ (01-075-1203), 9 = NaFeO₂ (04-007-6249), 10 = Na₂TiO₃ (00-037-0345) 10* Na₂TiO₃ (04-005-9405). The data are compared with the ICDD references in brackets.

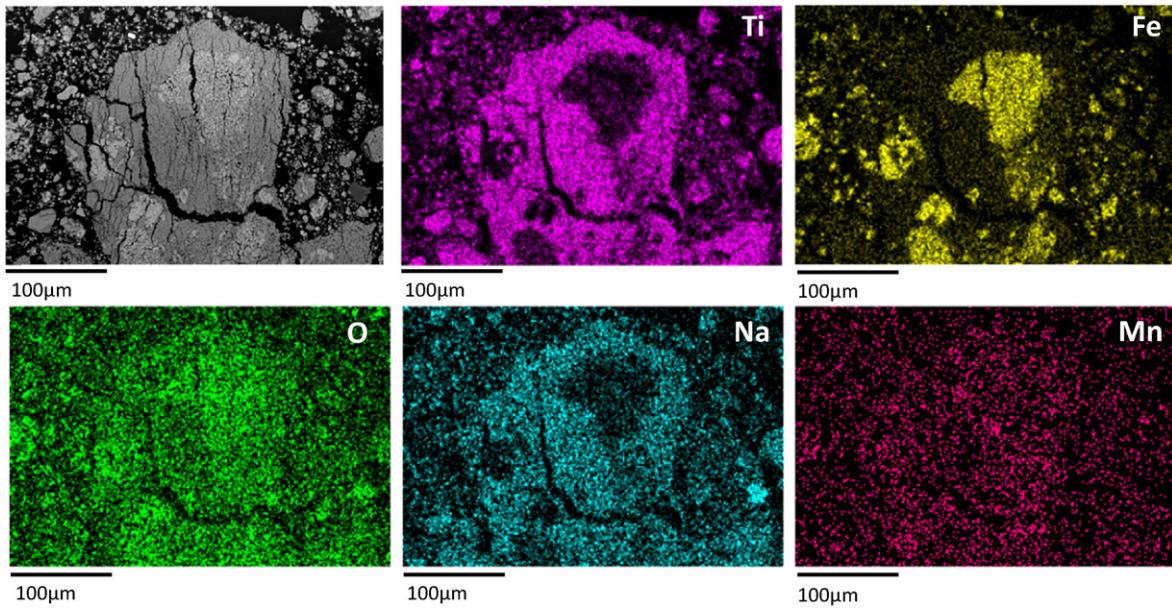
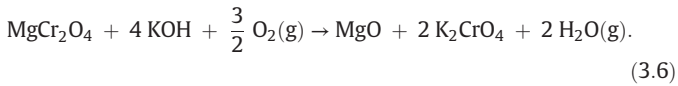
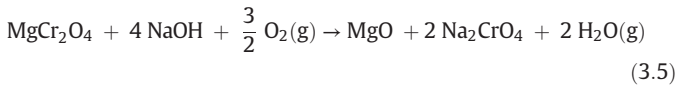
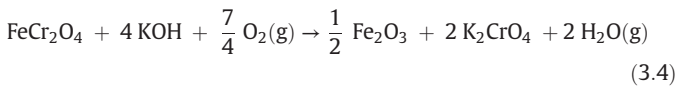
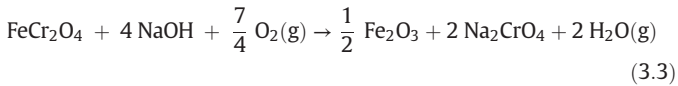


Fig. 12. Scanning electron microscopy elemental mapping images of water leached residue from ilmenite roasted with NaOH at 400 °C.

chromium-containing spinels during alkali roasting using either NaOH or KOH is summarised by reactions (3.3) to (3.6):



According to Fig. 9, the Gibbs energy values for KOH reactions (3.4) and (3.6), are more negative than the values for NaOH reaction (3.3) and (3.5), implying that the formation of K_2CrO_4 in oxidising atmosphere is more favourable.

The plot in Fig. 9 shows that, below 1300 °C, the Gibbs energy values for FeCr_2O_4 reactions are more negative than those for MgCr_2O_4 reactions. This indicates that MgCr_2O_4 is more stable than FeCr_2O_4 and thus harder to decompose below 1300 °C. Sun et al. (2007) explained the difference between the reactivity of iron and magnesium chromites in oxidising atmosphere taking into account the changes in the crystal structure due to the $\text{Fe}^{2+} \rightarrow \text{Fe}^{3+}$ oxidation step.

Both sodium and potassium hydroxides do not only react with chromite spinels but also combine with other spinel members and silicate impurities as shown in reactions (3.7) to (3.16).

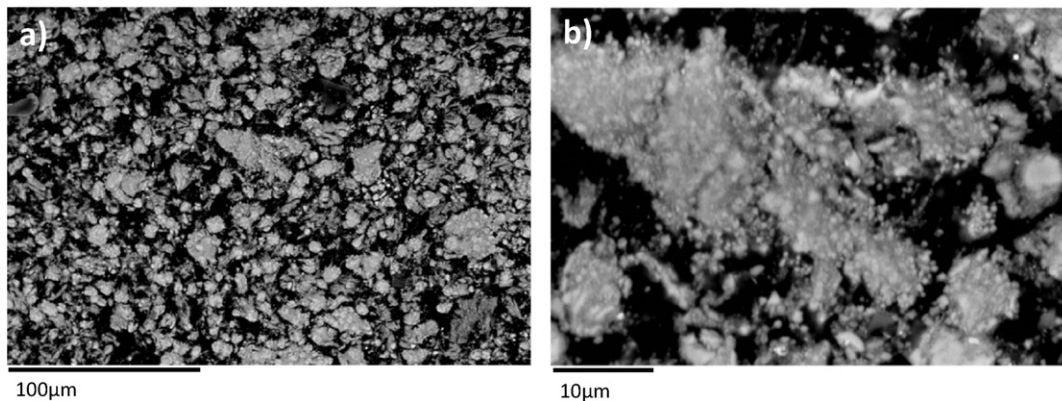
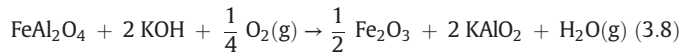
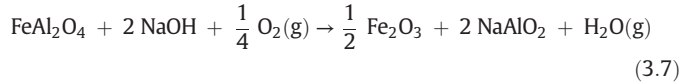
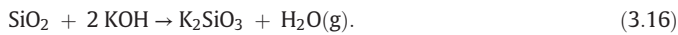
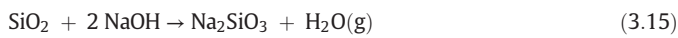
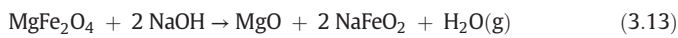


Fig. 13. Backscattered scanning electron microscopy elemental mapping images of water leached residue from ilmenite roasted with KOH at 400 °C: a) low magnification, b) high magnification.

Table 5

Chemical composition of roasted samples after two-stage leaching process. Samples were analysed by XRF.

wt. %	TiO ₂	Fe ₂ O ₃	Na ₂ O	K ₂ O	MnO	Al ₂ O ₃	SiO ₂
NaOH 400 °C	49.2	44.7	0.4	–	1.4	0.5	0.5
NaOH 700 °C	83.2	11.7	–	–	0.4	0.3	0.5
NaOH 1000 °C	84.7	13.6	–	–	0.4	0.6	0.7
KOH 400 °C	54.5	29.8	–	7.2	0.7	0.2	1.5
KOH 700 °C	62.4	30.7	–	1.7	0.6	1.1	1.3
KOH 1000 °C	43.8	34.4	–	13.1	1.1	2.4	0.9



By comparing ΔG values in Figs. 9 and 10, it is possible to deduce that the Na_2CrO_4 and K_2CrO_4 are more stable than the rest of phases formed via alkali roasting, e.g. NaAlO_2 , NaFeO_2 , Na_2SiO_3 , KAlO_2 , KFeO_2 and K_2SiO_3 . Note that ΔG figures for reaction (3.16) were not plotted as values are very positive (1343.97 kJ/mol, $T = 1000^\circ\text{C}$) and therefore not comparable with the rest of the reactions. The chromate phases form preferentially in comparison with the rest of alkali compounds, which favours the extraction of chromium from chromite spinel. However, previous research on thermodynamics of chromite ore roasting with soda-ash (Na_2CO_3) reported that reactions (3.7) to (3.16) do occur during the process. Tathavadkar et al. (2001) suggested the presence of these compounds during roasting of chromite ore with excess Na_2CO_3 and highlighted its adverse effect on oxygen diffusion by decreasing the eutectic temperature of the Na_2CO_3 - Na_2CrO_4 binary liquid. Qi et al. (2011) explained the thermodynamics of chromite roasting with Na_2CO_3 and proved the formation of these compounds (sodium ferrite, sodium aluminate and sodium silicates) during roasting, suggesting that they may act as intermediate compounds which can further react with chromite spinels to form sodium chromate. If we apply this to roasting of chromite with NaOH and KOH, and considering the excess alkali used in this study, then the formation

of sodium ferrite, aluminate and silicates are thermodynamically expected.

3.3. Processing of ilmenite minerals by alkali roasting and water leaching

The effects of roasting with NaOH and KOH were investigated by roasting ilmenite mineral samples at different temperatures (400 °C, 700 °C and 1000 °C) with excess of alkali ($\text{FeTiO}_3:\text{MOH} = 1:3.8$). XRPD patterns of roasted samples at 400 °C and 700 °C with both alkali salts are presented in Fig. 11.

When roasting at 400 °C the reactions do not appear to have gone to completion as some of the alkali salts remained in the roasted products for both KOH and NaOH, as seen in Fig. 11a and b, respectively. The phases formed when roasting with KOH at 700 °C were potassium titanate, potassium ferrite and potassium iron titanate, as observed in Fig. 11c. In Fig. 11d it can be seen that the phases formed during the roasting at 700 °C with NaOH are sodium titanate and sodium ferrite. The XRPD patterns presented in Fig. 11 depict the formation of alkali titanates and alkali ferrites, which agrees with findings by previous authors (Lahiri and Jha, 2009; Manhique et al., 2011).

Roasted samples were leached in hot water (60 °C) for 2 h. Iron, which remains as the main impurity, is present as a result of the hydrolysis of the alkali ferrites following reactions (3.17) to (3.19) and due to the formation of ternary phases (Foley and MacKinnon, 1970; Sanchez-Segado et al., 2015a). This was confirmed due to the increase in pH that was observed during the water leaching stage.



The effect of roasting with NaOH and KOH was studied at different temperatures (400 °C, 700 °C and 1000 °C) with excess of alkali ($\text{FeTiO}_3:\text{MOH} = 1:3.8$). Roasted samples were leached in hot water (60 °C) for 2 h.

The water leached residues were analysed by SEM. Fig. 12 shows that roasting with NaOH at 400 °C results in extensive transgranular cracks throughout the ilmenite structure. This is likely due to a significant partial pressure of H_2O during the roasting experiments (Sanchez-Segado et al., 2015a). The partial pressure of water for roasting with NaOH at 400 °C (reaction (3.2)) was calculated to be 5.62×10^8 atm. These cracks promote the diffusion of the Na^+ ions throughout the structure, leading to the formation of sodium titanate. At temperatures below 550 °C binary phases of sodium titanate and sodium ferrite (Manhique et al., 2011) form. This process leads to the segregation of iron oxide from sodium titanate, as seen in Fig. 12. The iron present here is likely due to the

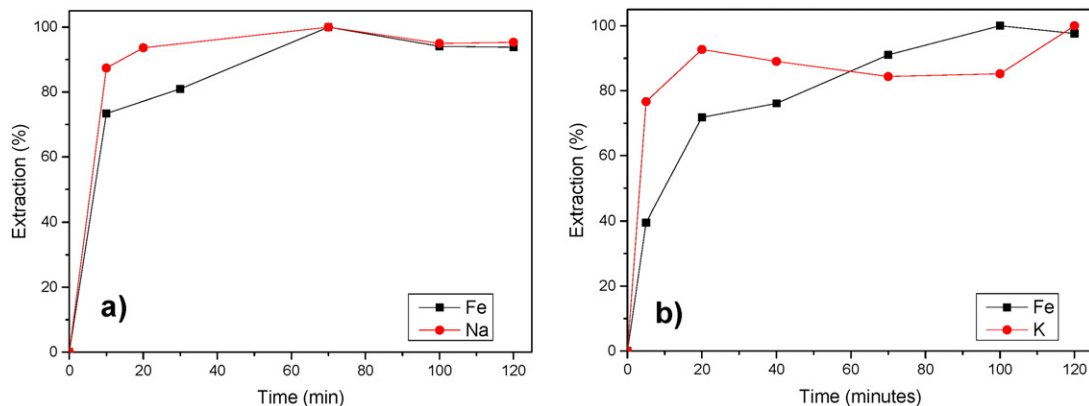


Fig. 14. Extraction of metals versus time during the acid leaching stage: a) ilmenite roasted with NaOH at 700 °C and b) ilmenite roasted with KOH at 700 °C.

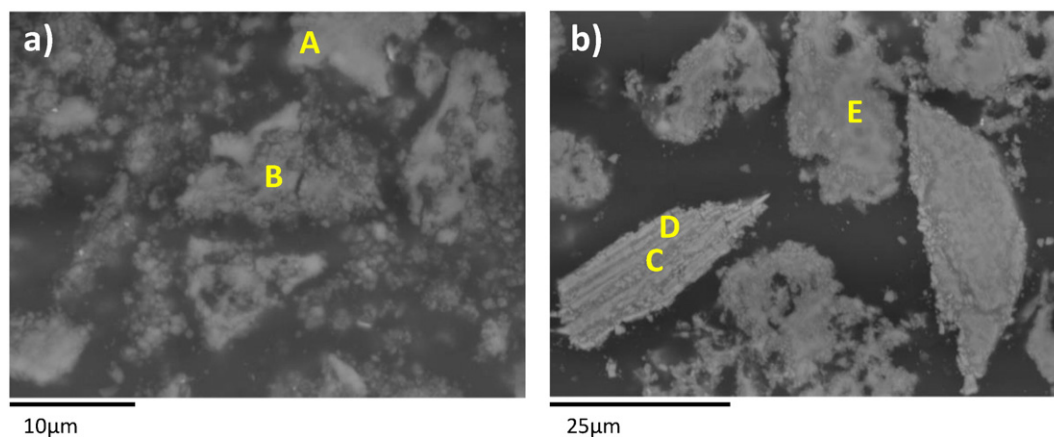


Fig. 15. Backscattered images of two-stage leaching residues: a) ilmenite roasted with NaOH at 700 °C and b) ilmenite roasted with KOH at 700 °C.

hydrolysis of the sodium ferrite, as described in reaction (3.18). A pH increase during the water leaching confirms reactions (3.17) to (3.19). The SEM results in Fig. 12 broadly agree with the E_h -pH diagram presented in reference (Lahiri and Jha, 2009). It is also likely that the NaOH has reacted with pseudorutile phase to form sodium titanate on the periphery of the particle.

In Fig. 13, the SEM of the water leached residue after roasting with KOH at 400 °C shows that these particles have depicted a different microstructure when compared to those roasted with NaOH. When roasting with KOH the particles have a cotton-seed like morphology, unlike the transgranular cracks observed when roasting with NaOH. It is also clear that there is limited segregation between iron and titanium, suggesting the formation of a ternary phase of potassium iron titanate, where potassium ions substituted titanium and/or iron atoms present in the ilmenite lattice (Manhique et al., 2011). This potassium iron titanate phase was also observed in the XRPD pattern (Fig. 11a) of the roasted sample before water leaching. KOH has reacted with ilmenite by forming K-Ti-Fe-O (K = 10%, Ti = 32.7%, Fe = 26.3%, O = 25.9%) ternary phase which was analysed by SEM-EDX analysis as (K = 10%, Ti = 32.7%, Fe = 26.3%, O = 25.9%). The K-Ti-Fe-O ternary oxide did not decompose into potassium titanate and potassium ferrite.

3.3.1. Formation of high grade TiO_2

In order to determine the optimal conditions for the upgrading of the TiO_2 content by organic acid leaching, the E_h -pH diagrams of the K-Ti-Fe-O-H and the Na-Ti-Fe-O-H systems presented by other authors (Lahiri, 2010; Ephraim and Jha, 2015) were studied. These have shown that the optimal conditions are achieved when the pH is below 4, in slightly reducing conditions. For these reasons, a mixture of oxalic acid and ascorbic acid was used during the acid leaching stage. Ascorbic acid was used for its known reduction potential (Suter et al., 1991).

Table 5 shows the TiO_2 content of the residues after the roasting and two-stage (water and acid) leaching process. It is clear from this table that the TiO_2 content after roasting with NaOH is higher compared with KOH roasting. Recovery of TiO_2 increases with temperature for samples roasted with NaOH, as seen in the table. This is because of the

increasing tendency for the formation of sodium titanate and sodium ferrite as observed by other authors (Lahiri and Jha, 2007). The presence of iron in the samples roasted with NaOH may be due to the presence of unreacted ilmenite, as this phase was observed in the XRPD pattern for the sample roasted with NaOH at 700 °C and then leached with organic acid (Fig. 16). However, the maximum recovery was achieved at 700 °C but it decreased at 1000 °C for the sample roasted with KOH. The decreased recovery of TiO_2 was caused by formation of a complex less soluble K-Fe-Ti-O phase. Even though previous authors have been leaching the samples for several hours (>4 h) our leaching time was limited to 2 h. Short leaching times may save a lot of time and increase production and hence requires investigation (Sanchez-Segado et al., 2015a).

After water leaching of the ilmenite roasted at 700 °C, the resulting residues were leached with the organic acid mixture. A sample of the acid leach solution was taken at different time intervals for analysis by AAS, in order to study the extraction of key metals (Fe, Na and K) with time. The AAS results from samples roasted at 700 °C are presented in Fig. 14. Fig. 14a shows the extraction of iron and sodium during the course of the organic acid leaching, while Fig. 14b shows the extraction of iron and potassium. In Fig. 14a, the extraction of both metals begins rapidly with the reaction being almost complete after 80 min. In Fig. 14b, the curve has a similar profile to that observed in Fig. 14a.

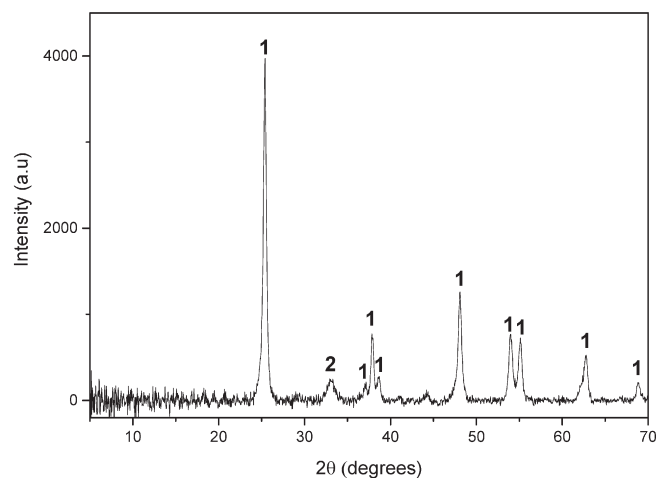


Fig. 16. XRPD pattern of residue of ilmenite roasted at 700 °C and then water and acid leached. 1 = Anatase (TiO_2) (04-002-2751), 2 = Ilmenite ($FeTiO_3$) (04-012-1150). The data are compared with the ICDD references in brackets.

Table 6
Elemental composition of areas A to E in Fig. 15 analysed by SEM-EDX.

%wt.	Ti	Fe	O	Mn	Na	K	Si	Ca	Al	V
A	47.6	11.7	40.0	0.4	–	–	0.4	–	–	–
B	52.2	5.7	39.7	0.8	0.7	–	–	0.7	0.2	–
C	33.5	38.5	24.6	1.5	–	0.1	0.4	0.8	0.1	0.4
D	33.3	37.5	27.5	1.6	–	–	–	0.2	–	–
E	38.0	26.2	33.3	–	–	1.5	0.4	0.6	–	–

Table 7

Wt.% Cr₂O₃ in the water leached residues after roasting of chromite with NaOH or KOH at different temperatures. Samples were analysed by XRF.

Chromium left in the solid residues after water leaching (wt. %Cr ₂ O ₃)	
<i>Chromite + NaOH</i>	
400 °C	46.3
700 °C	24.7
1000 °C	3.65
<i>Chromite + KOH</i>	
400 °C	39.7
700 °C	24.5
1000 °C	3.73

The SEM images of the residues after the two-stage leaching process were analysed by EDX and the results are presented in Fig. 15 and Table 6. Fig. 15a shows that the TiO₂ particles are fine and iron, the major impurity, is present in solid solution with the TiO₂, which is confirmed by observing Table 6.

The two-stage leaching of the ilmenite roasted with KOH clearly did not produce TiO₂ of the same quality when compared to NaOH, according to results presented in Table 5. The removal of iron and alkali is less when compared to the NaOH experiments. SEM analysis of the acid leach residue in Fig. 15b shows that the iron and titanium are present together as FeTiO₃. The final residue after ilmenite roasting with NaOH at 700 °C and the two-stage leaching process is presented in Fig. 16, from which it is evident that the dominant phase is anatase and the remaining impurity is iron, present as ilmenite. Further optimisation of the roasting chemistry is necessary in order to avoid unreacted ilmenite and maximise the final TiO₂ yield.

3.4. Processing of chromite ore by alkali roasting and water leaching

Chromite ore was roasted with excess NaOH or KOH in air atmosphere at three different temperatures, 400 °C, 700 °C and 1000 °C. Roasted samples were water leached for 2 h at 60 °C. A summary of

the experiments carried out is presented in Table 2. Water leached residues were analysed by XRF and XRPD in order to quantify the residual chromium and the main phases present. The results are presented in Table 7 and Fig. 17.

It can be seen from Table 7 that chromite spinel does not undergo significant decomposition when roasted with alkali at 400 °C. This is corroborated by XRPD patterns in Fig. 17, where it can be seen that chromite spinel is the main phase in the water leached residues after roasting at 400 °C with both hydroxides. According to Table 7, potassium hydroxide seems to be more reactive than sodium hydroxide at low temperature. However, above 400 °C small differences in the extraction yield were found which justify the use of sodium hydroxide because of its lower price. In Fig. 18a, a backscattered SEM image of a water leached residue after chromite roasting with KOH at 400 °C is presented, from which it is apparent that chromite particles remained unreacted.

When the reaction is carried out at 700 °C, the percentage of chromium in the residue is still significantly high at 24.7 wt.% Cr₂O₃ for NaOH and 24.5 wt.% Cr₂O₃ for KOH, indicating that the chromite structure was not completely destroyed at this temperature. Looking at the structure of the water leached residue particles after roasting of chromite with KOH at 700 °C, presented in Fig. 18b, a partially reacted chromite core (bright phase) depleted in chromium can be observed. This is confirmed by the XRPD patterns for KOH at 700 °C (Fig. 17) where Mg–Fe–Al and Mg–Cr–Al spinel phases are present. The SEM image shows that the core is surrounded by a reaction layer (darker phase). The Shrinking-core model has been applied to the chromite roasting by previous authors (Xu et al., 2006).

At 1000 °C, chromite ore reacted to a significant extent with alkali and most chromium was extracted as sodium or potassium chromate by water leaching. The wt.% of Cr₂O₃ decreased from 48.8% in the as-received chromite sample to 3.65% and 3.73% in the water leached residues after roasting with sodium and potassium hydroxides, respectively.

During alkali roasting, the Cr³⁺ cations diffuse towards the reaction zone where they combine with Na⁺/K⁺ to form water-soluble

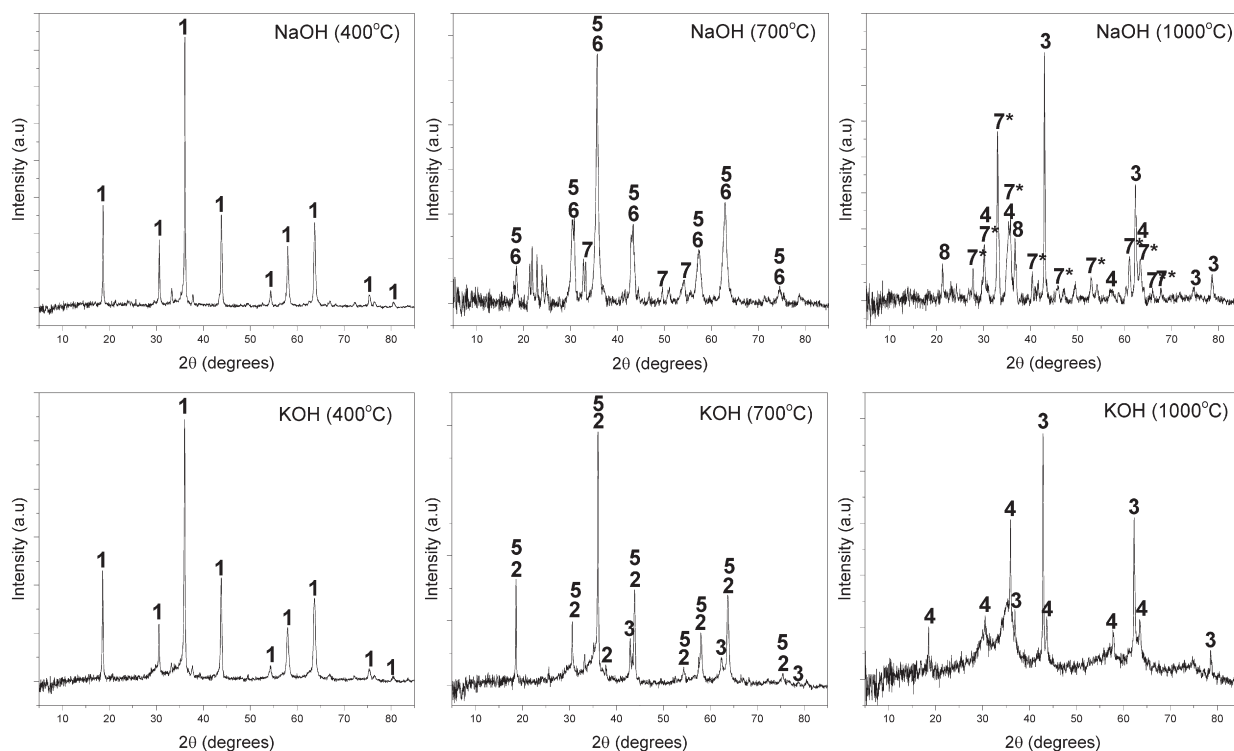


Fig. 17. XRPD patterns of water leached residues after chromite ore roasting with NaOH and KOH at 400 °C, 700 °C and 1000 °C. 1 = (Mg,Fe)(Cr,Al)₂O₄ (00-009-0353), 2 = Mg(Fe_{0.5}Al_{0.5})₂O₄ (01-080-3017), 3 = MgO (04-002-5660), 4 = MgFe₂O₄ (04-012-1065), 5 = MgCrAlO₄ (04-006-0491), 6 = (MgAl_{0.74}Fe_{1.26})₂O₄ (01-088-0867), 7 = Fe₂O₃ (04-008-7623), 7* = Fe₂O₃ (00-052-1449), 8 = Na_{1.15}Al_{1.15}Si_{0.85}O₄ (00-049-0007). The data are compared with the ICDD references in brackets.

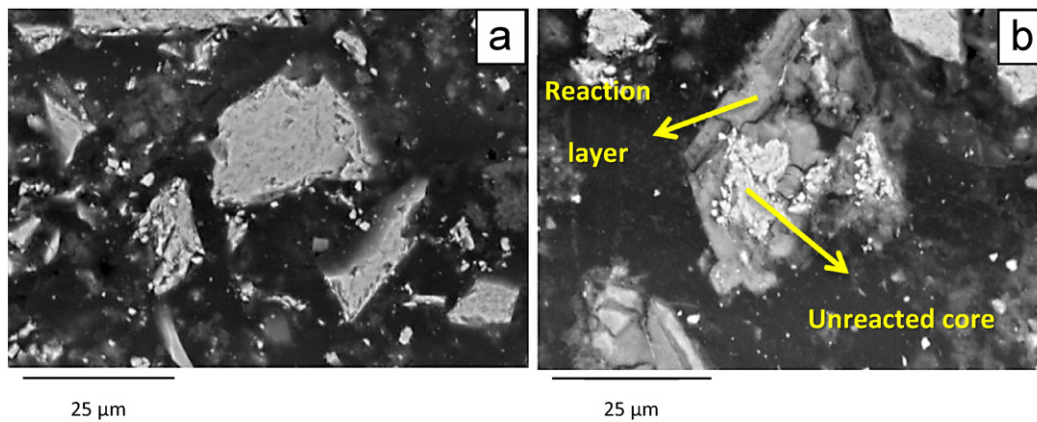


Fig. 18. Backscattered SEM images of water leached residues after roasting of chromite ore with KOH at a) 400 °C and b) 700 °C.

chromate compounds (Na_2CrO_4 , K_2CrO_4) which are subsequently extracted during water leaching. Aluminium is also leached out in the form of water-soluble alkali aluminates (NaAlO_2 , KAlO_2). Consequently, the remaining residue after water leaching is Fe and Mg-rich. A backscattered SEM image of a water leached residue after chromite roasting with NaOH at 1000 °C is shown in Fig. 19. Tathavadkar et al. (2003) described how Mg^{2+} cations diffuse outwards from the chromite structure during the soda-ash roasting of South African chromite, occupying voids in the Fe-rich phase surrounding the unreacted core and promoting the formation of magnesioferrite (MgFe_2O_4). Magnesioferrite formation is also observed when chromite is roasted with NaOH and KOH. The XRPD pattern of the water leached residue after roasting with NaOH at 1000 °C, in Fig. 17, confirms the presence of MgFe_2O_4 , but Fe_2O_3 and MgO phases can also be found separately. SEM elemental mapping of the same sample presented in Fig. 19 clearly shows Fe_2O_3 and MgO phase segregation. This may be explained by the excess alkali present during the roasting reaction, which leads to water-soluble NaFeO_2 formation.

Reaction (3.20) shows the formation of NaFeO_2 by reaction of MgFe_2O_4 with NaOH. The Gibbs energy value for this reaction at 1000 °C, computed using HSC 5.1 software (Roine and Outokumpu, 2002), is -27.6 kJ per mol of MgFe_2O_4 reacted, which indicates that MgFe_2O_4 may react with excess alkali to form MgO and water-soluble NaFeO_2 when roasting is carried out at 1000 °C:



During water leaching, the separation of NaFeO_2 into NaOH and Fe_2O_3 takes place, followed by precipitation of iron oxide which remains

in the residue. This was also described in the previous section for water leaching of alkali roasted ilmenite samples. The main phases found in the residue after water leaching are MgO, Fe_2O_3 , MgFe_2O_4 and sodium aluminium silicate, as shown in the XRPD pattern in Fig. 17. Some free silica is also observed, as apparent from the elemental mapping in Fig. 19.

3.4.1. Roasting time effect on chromium extraction

Chromite ore samples were roasted with NaOH and KOH at 1000 °C for different periods of time (15 min to up to 2 h) and subsequently water leached for 2 h at 60 °C. The molar ratio Cr_2O_3 :MOH was kept constant at 1:7.8. The XRF analysis of the residues after water leaching was used to calculate the extraction yield according to the equation below. Chromium extraction profiles are presented in Fig. 20.

$$\text{Extraction yield (\%)} = \frac{\text{Cr in chromite} - \text{Cr in residue}}{\text{Cr in chromite}} * 100.$$

During the early stages of reaction, extraction kinetics is slower for NaOH compared with KOH reaction as shown in Fig. 20, which might be due to extensive fracture of particles caused by potassium ions. The fractured surface area is larger in K^+ ions than with Na^+ ions (Sanchez-Segado et al., 2015b). Eventually, the two extraction curves converge and the final chromium extraction is quite similar for both the hydroxides, yielding slightly above 95% extraction efficiency at 1000 °C for 2 h, respectively.

A SEM micrograph and line scan analysis of a water-leached sample previously roasted with NaOH at 1000 °C for 30 min can be seen in Fig. 21a. After 30 min of reaction, a clearly defined reaction layer can

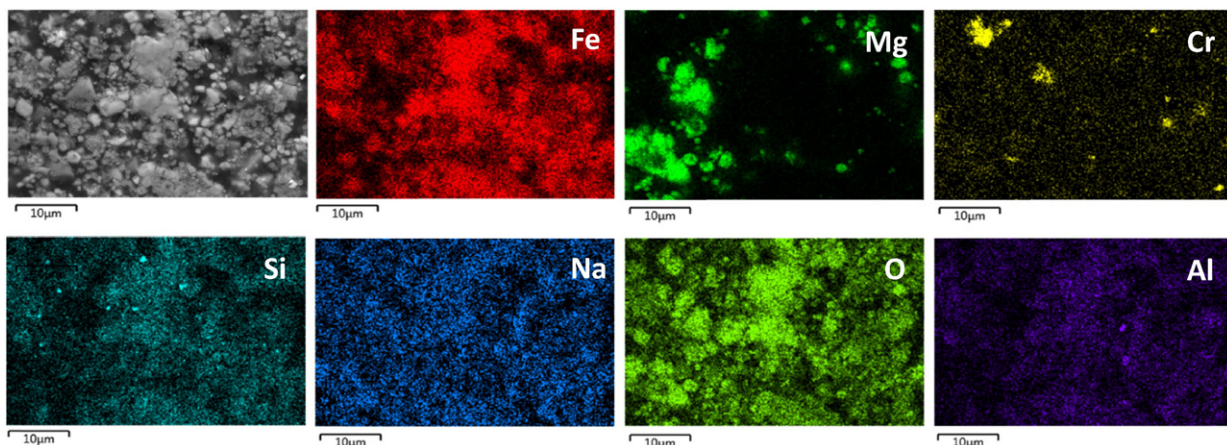


Fig. 19. Backscattered SEM image and elemental mapping of a water leached residue after chromite ore roasting with NaOH at 1000 °C.

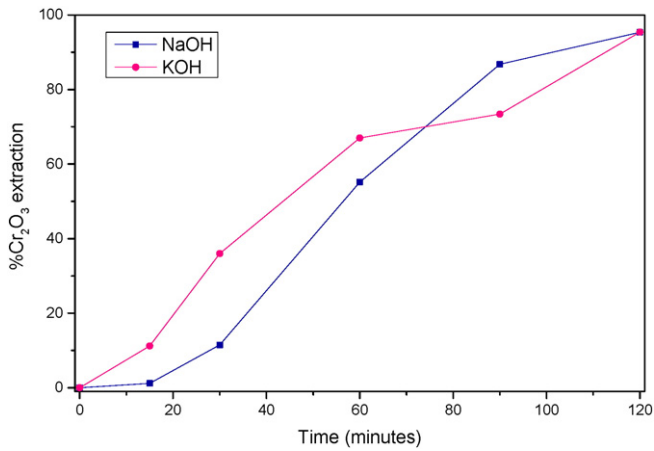


Fig. 20. Influence of time over chromium extraction yield for samples roasted at 1000 °C ($\text{Cr}_2\text{O}_3:\text{MOH} = 1:7.8$) and water leached at 60 °C.

be differentiated from the unreacted chromite core. The reaction product is composed of two distinct phases, an inner layer surrounding the unreacted core and an outer layer. The difference in colour intensity of the two rings indicates that there is a difference in chemical composition between them, which was confirmed by line scan and chemical analysis of the particle using EDX. The chemical composition of the three distinct areas indicated in Fig. 21b was also analysed by SEM–EDX, presented in Table 8.

Table 8

Elemental composition of unreacted core, inner and outer product layers indicated in Fig. 21b analysed by SEM–EDX.

wt.%	Cr	Fe	O	Mg	Al	Si	Ca	Na	Ti
Unreacted core	32.7	19.7	31.4	6.8	9	–	–	–	0.4
Inner layer	45.3	12.7	25.5	1.6	6.8	–	0.2	7.5	0.5
Outer layer	31.7	22.6	23.6	6.0	2.3	0.6	0.6	12.4	0.3

Line scan in Fig. 21b shows how both chromium and aluminium concentrations progressively decrease as you move towards the reaction interface, where reaction with alkali forms water-soluble Na_2CrO_4 and NaAlO_2 . In the first stages of the reaction, the oxidation of Fe^{2+} present in the chromite spinel to Fe^{3+} occurs, via voids generated in the spinel structure as a consequence of this oxidation process (Tathavakar et al., 2005). These structural vacancies promote the diffusion of Cr^{3+} outwards the chromite grain. Iron diffuses from the chromite spinel structure to the reaction layer, where it can mainly be found in the outer ring not in the inner one as seen in the Fe line scan graph in Fig. 21b. Magnesium ions are present in the outermost part of the reaction layer and are likely to combine with iron to form MgFe_2O_4 .

This is in agreement with the elemental analysis shown in Table 8, where it can be seen how Fe and Mg are more concentrated in the outer layer than in the inner one. The results show that the wt.% of chromium in the inner layer is higher, which can be due to the relatively lower concentration of Fe and Mg.

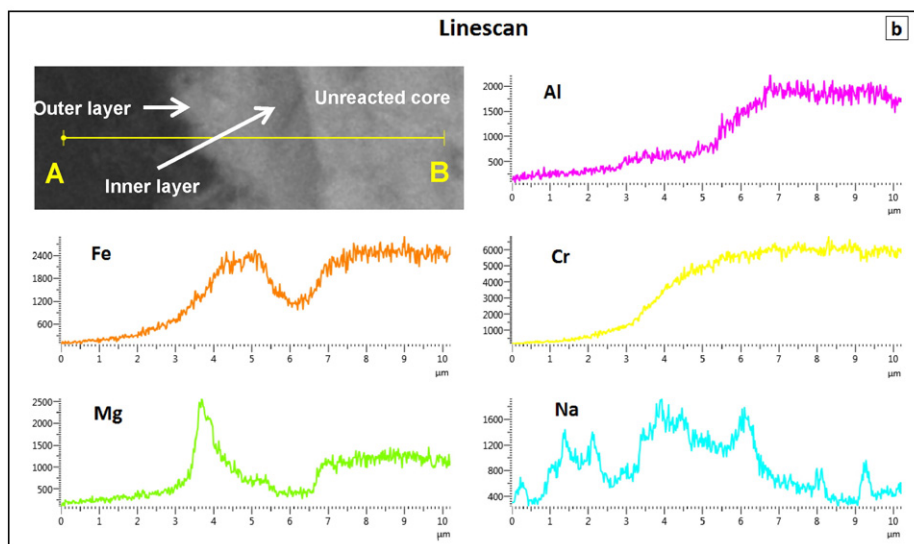
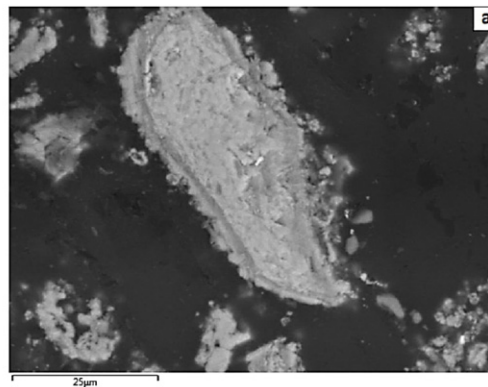


Fig. 21. a) Backscattered SEM image of a residue particle after chromite roasting with NaOH at 1000 °C for 30 min and water leaching and b) line-scan analysis from points A to B in a higher magnification area.

4. Conclusions

- Characterisation of as-received samples showed that the South African chromite ore used in this study is constituted by a solid solution of FeCr_2O_4 , MgCr_2O_4 , FeAl_2O_4 and MgAl_2O_4 . The main phase identified by XRPD was $(\text{Fe}_{0.52}\text{Mg}_{0.48})(\text{Cr}_{0.76}\text{Al}_{0.24})_2\text{O}_4$, with calcium and aluminium silicates and free silica also present as gangue. Characterisation of the as-received ilmenite indicated that it was primarily composed of ilmenite (FeTiO_3) and pseudorutile ($\text{Fe}_2\text{Ti}_3\text{O}_9$), a weathered phase from ilmenite.
- Comparison of the roasting process thermodynamics for chromite and ilmenite highlights some similarities. The main conclusion obtained is that the roasting step is thermodynamically more favourable when using KOH as compared to NaOH, for both ilmenite and chromite.
- In the case of ilmenite, it was observed that treatment with NaOH yielded better results when compared with KOH. The maximum purity of TiO_2 obtained when using NaOH was 84 wt.% TiO_2 , whereas 62.5 wt.% TiO_2 was the maximum obtained when using KOH. These residues were obtained after a shortened leaching time of 2 h. Optimisation of alkali roasting is needed to improve the purity of TiO_2 obtained. For chromite treatment, the results for both hydroxides were found to be comparable, achieving 95.3% and 95.4% of Cr extraction for NaOH and KOH, respectively, when roasting at 1000 °C for 2 h and water leaching.
- The extraction yield of TiO_2 increases with the roasting temperature up to 700 °C. Above 700 °C, for NaOH the temperature had a negligible effect. Meanwhile, for KOH the increased temperature had a negative effect on the grade of TiO_2 obtained. This was different for chromite roasting where at 700 °C a significant amount of unreacted chromite was still present; while at 1000 °C, the reaction with both alkali salts was almost complete with a remaining processing residue containing a maximum value of 3.7 wt.% Cr_2O_3 .
- At 1000 °C, KOH was found to be more reactive during the initial stages of chromite ore roasting, giving a better extraction yield than NaOH up to approximately 70 min. After this point, the extraction curves converge resulting in a similar extraction yield after 2 h.

Acknowledgements

The authors acknowledge the financial support from the EPSRC standard grants (GR/T08074/01 and GR/L95977/01) and PhD studentships for research which were initiated in 1997 at the University of Leeds. AJ also acknowledges the support from the European Union's Marie Curie Fellowship grant number 331385 for Dr. Sanchez-Segado and from the NERC's Catalyst Grant reference NE/L002280/1.

References

Amer, A.M., 2002. Alkaline pressure leaching of mechanically activated Rosetta ilmenite concentrate. *Hydrometallurgy* 67 (1–3), 125–133.

Antony, M., et al., 2001. The soda-ash roasting of chromite ore processing residue for the reclamation of chromium. *Metall. Mater. Trans. B* 32 (6), 987–995.

Antony, M., Jha, A., Tathavadar, V., 2006. Alkali roasting of Indian chromite ores: thermodynamic and kinetic considerations. *Miner. Process. Ext. Metall.* 115 (2), 71–79.

Arslan, C., Orhan, G., 1997. Investigation of chrome (VI) oxide production from chromite concentrate by alkali fusion. *Int. J. Miner. Process.* 50 (1), 87–96.

Becher, R., et al., 1965. A new process for upgrading ilmenitic mineral sands. *Australasian Inst Mining Met Proc.*

Brown, T., et al., 2015. *World Mineral Production 2009–2013*. British Geological Survey.

Burns, R.G., 1993. *Mineralogical Applications of Crystal Field Theory* Vol. 5. Cambridge University Press.

Ding, Y., Ji, Z., 2003. *Production and Application of Chromium Compounds*. Press of Chemical Industry, Beijing.

Ephraim, J.K., Jha, A., 2015. Leaching studies of alkali roasted bomarilmenite and anatase during the processing of synthetic rutile. *Hydrometallurgy* 152, 113–119.

Farrow, J., Ritchie, I., Mangano, P., 1987. The reaction between reduced ilmenite and oxygen in ammonium chloride solutions. *Hydrometallurgy* 18 (1), 21–38.

Filippou, D., Hudon, G., 2009. Iron removal and recovery in the titanium dioxide feedstock and pigment industries. *JOM* 61 (10), 36–42.

Foley, E., MacKinnon, K.P., 1970. Alkaline roasting of ilmenite. *J. Solid State Chem.* 1 (3–4), 566–575.

Geveci, A., Topkaya, Y., Ayhan, E., 2002. Sulfuric acid leaching of Turkish chromite concentrate. *Miner. Eng.* 15 (11), 885–888.

Grey, I., Reid, A., 1975. The structure of pseudorutile and its role in the natural alteration of ilmenite. *Am. Mineral.* 60 (9/10), 179–181.

Habashi, F., 1997. *Handbook of Extractive Metallurgy*. John Wiley & Sons.

Hundley, G.L., Nilsen, D., Siemens, R.E., 1985. *Extraction of Chromium From Domestic Chromites by Alkali Fusion* Vol. 8977. US Department of the Interior, Bureau of Mines.

Klein, C., Philpotts, A., 2012. *Earth Materials: Introduction to Mineralogy and Petrology*. Cambridge University Press.

Kogel, J.E., 2006. *Industrial Minerals & Rocks: Commodities, Markets, and Uses*. SME.

Kowalski, Z., Gollinger-Tarajko, M., 2003. Environmental evaluation of different variants of the chromium compound production model using chromic waste. *Waste Manag.* 23 (8), 771–783.

Lahiri, A., 2010. Influence of ascorbate and oxalic acid for the removal of iron and alkali from alkali roasted ilmenite to produce synthetic rutile. *Ind. Eng. Chem. Res.* 49 (18), 8847–8851.

Lahiri, A., Jha, A., 2007. Kinetics and reaction mechanism of soda ash roasting of ilmenite ore for the extraction of titanium dioxide. *Metall. Mater. Trans. B* 38 (6), 939–948.

Lahiri, A., Jha, A., 2009. Selective separation of rare earths and impurities from ilmenite ore by addition of K^+ and Al^{3+} ions. *Hydrometallurgy* 95 (3–4), 254–261.

Mackey, T.S., 1994. Upgrading ilmenite into a high-grade synthetic rutile. *JOM* 46 (4), 59–64.

Maliotis, G., 1996. *Chromium uses and markets*. Statistical supplement.

Manhique, A.J., Focke, W.W., Madivate, C., 2011. Titania recovery from low-grade titaniferous minerals. *Hydrometallurgy* 109 (3–4), 230–236.

Nayl, A.A., Aly, H.F., 2009. Acid leaching of ilmenite decomposed by KOH. *Hydrometallurgy* 97 (1–2), 86–93.

Nickens, K.P., Patierno, S.R., Ceryak, S., 2010. Chromium genotoxicity: a double-edged sword. *Chem. Biol. Interact.* 188 (2), 276–288.

Pauling, L., 1929. The principles determining the structure of complex ionic crystals. *J. Am. Chem. Soc.* 51 (4), 1010–1026.

Qi, T.-g., et al., 2011. Thermodynamics of chromite ore oxidative roasting process. *J. Cent. S. Univ. Technol.* 18, 83–88.

Roine, A., Outokumpu, H., 2002. *Chemistry for Windows: Chemical Reaction and Equilibrium Software with Extensive Thermodynamical Database, Version 5.1, User's Guide*. Outokumpu Research Oy, Finland.

Rosenbaum, J.B., 1982. Titanium technology trends. *JOM* 34 (6), 76–80.

Sanchez-Segado, S., Jha, A., 2013. Physical chemistry of roasting and leaching reactions for chromium chemical manufacturing and its impact on environment – a review. *Materials Processing Fundamentals*. John Wiley & Sons, Inc., pp. 225–236.

Sanchez-Segado, S., Lahiri, A., Jha, A., 2015a. Alkali roasting of bomarilmenite: rare earths recovery and physico-chemical changes. *Open Chem.* 13 (1).

Sanchez-Segado, S., et al., 2015b. Reclamation of reactive metal oxides from complex minerals using alkali roasting and leaching – an improved approach to process engineering. *Green Chem.* 17 (4), 2059–2080.

Sun, Z., Zheng, S., Zhang, Y., 2007. Thermodynamics study on the decomposition of chromite with KOH. *Acta Metall. Sin. (Engl. Lett.)* 20 (3), 187–192.

Suter, D., Banwart, S., Stumm, W., 1991. Dissolution of hydrous iron(III) oxides by reductive mechanisms. *Langmuir* 7 (4), 809–813.

Tathavadar, V., Jha, A., Antony, M., 2001. The soda-ash roasting of chromite minerals: kinetics considerations. *Metall. Mater. Trans. B* 32 (4), 593–602.

Tathavadar, V.D., Jha, A., Antony, M., 2003. The effect of salt-phase composition on the rate of soda-ash roasting of chromite ores. *Metall. Mater. Trans. B* 34 (5), 555–563.

Tathavadar, V., Antony, M., Jha, A., 2004. An investigation of the mineralogical properties of chemical grade chromite minerals. *Scand. J. Metall.* 33 (2), 65–75.

Tathavakar, V.D., Antony, M., Jha, A., 2005. The physical chemistry of thermal decomposition of South African chromite minerals. *Metall. Mater. Trans. B* 36 (1), 75–84.

Tel'pish, V., Vil'nyanskii, Y.E., 1969. Kinetics of sodium chromate formation during roasting of chromite charges. *J. Appl. Chem. USSR* 42, 1118–1120.

Teufer, G., Temple, A.K., 1966. Pseudorutile—a new mineral intermediate between ilmenite and rutile in the N alteration of ilmenite. *Nature* 211 (5045), 179–181.

U.S. Geological Survey, 2015. *Mineral Commodity Summaries*. Chromium. USGS, Virginia, pp. 42–43.

Wilson, N.C., et al., 2005. Structure and properties of ilmenite from first principles. *Phys. Rev. B* 71 (7), 075202.

Xu, H.-B., et al., 2005. Oxidative leaching of a Vietnamese chromite ore in highly concentrated potassium hydroxide aqueous solution at 300 °C and atmospheric pressure. *Miner. Eng.* 18 (5), 527–535.

Xu, H.-B., et al., 2006. Development of a new cleaner production process for producing chromic oxide from chromite ore. *J. Clean. Prod.* 14 (2), 211–219.

Zhang, Y., et al., 2010. Effect of mechanical activation on alkali leaching of chromite ore. *Trans. Nonferrous Metals Soc. China* 20 (5), 888–891.

Zhang, W., Zhu, Z., Cheng, C.Y., 2011. A literature review of titanium metallurgical processes. *Hydrometallurgy* 108 (3–4), 177–188.

Zhao, Q., et al., 2014. Sulfuric acid leaching of South African chromite. Part 1: study on leaching behavior. *Int. J. Miner. Process.* 130, 95–101.